Transverse Recirculating-BBU Threshold Current in the Cornell x-ray ERL

Changsheng Song and Georg H. Hoffstaetter
Laboratory of Elementary Particle Physics, Cornell University

June 5, 2006

Abstract

The total current that can be accelerated in an Energy Recovery Linear Accelerator (ERL) can be limited by the transverse recirculating beam-breakup instability (BBU). A one-dimensional analysis of BBU is possible if the transverse optics does not couple vertical (y) and horizontal (x) oscillations and the higher-order dipole modes (HOMs) of the accelerating cavities are unpolarized or all polarized in the y and x directions. However, the threshold current can be increased if a totally coupled optics is used. In such an optics, beam oscillations in x during the first pass through the linac are converted into y oscillations for the second pass, and vice versa.

Here we analyze how much the BBU threshold current can be increased by using polarized HOMs and a coupled optics for the x-ray ERL being designed at Cornell University. This analysis will show: (a) how many HOMs have to be considered in the simulation of threshold currents, (b) by how much the threshold current is increased if there is a frequency spread between HOMs of the more than 300 cavities of the x-ray ERL and how much frequency spread is sufficient, (c) by how much the threshold current is increased by using polarized modes and a coupled optics and by how much x and y HOM frequencies have to be separated, (d) by how much does the threshold current increase if a frequency spread as well as polarized modes with coupled optics are used, (f) how the simulated threshold currents are distributed for a random distribution of HOM frequencies.

1 Introduction

In an Energy Recovery Linac the electron beam goes through the RF cavities more than once. Each electron bunch first passes the linac's cavities for its acceleration, and after a return loop it enters the linac a second time for the bunch's deceleration. When the beam returns to the same linac for acceleration several times and then is brought back for deceleration several times, one refers to a multi-turn ERL. However, here we will analyze the single-turn ERL that is being planned at Cornell University where a 100mA beam is to be accelerated up to an energy of 5GeV, at which it is used to generate highly-brilliant x-ray beams.

The return of the electron beam for a second pass through the linac can incur the transverse beam-breakup instability. A simplified picture for BBU is the following: when an electron bunch gets a transverse kick by HOMs in a cavity, it will return to this cavity during its second pass through the linac with a transverse displacement, which may pump more energy into the HOMs. If HOMs get enhanced by the bunch on its second pass, they may kick the next bunch even harder. When the current becomes so large that more energy is transfered into a HOM by bunches than is taken out by HOM couplers, the HOM power will start to grow exponentially. This process will eventually cause a loss of the beam.

If we assume that HOMs behave independently and do not interfere with each other, we can get an approximate formula of the threshold current in the presence of a single higher order mode [1, 2, 3],

$$I_{\mathrm{th}} = -\frac{\omega_\lambda}{e\left(\frac{R}{Q}\right)_\lambda Q_\lambda}\frac{1}{T_{12}^* \sin\omega_\lambda t_r} \tag{1}$$

$$T_{12}^* = T_{12}\cos^2\theta_\lambda + \frac{T_{14}+T_{32}}{2}\sin 2\theta_\lambda + T_{34}\sin^2\theta_\lambda \tag{2}$$

where $(R/Q)_\lambda$ is the shunt impedance, Q_λ is the quality factor, θ_λ is the polarization angle from the x direction, ω_λ is the HOM frequency and t_r is the bunch return time, e is the elementary charge and the matrix $\mathbf{T}$ describe how a transverse momentum is transported to a transverse displacement after one turn. From this formula we can see that a small Q_λ or $(R/Q)_\lambda$ can increase the threshold current. A small Q_λ indicates a short damping time. Therefore

Table 1: The four dominant transverse HOMs for the 7-cell ERL cavity in the circuit definition.

	f_λ(GHz)	Q_λ	$(R/Q)_\lambda[\Omega/\mathrm{m}^2]$	$(R/Q)_\lambda[\Omega]$
1	1.87394	20912.4	84409.3	109.60
2	1.88173	13186.1	21629.3	27.85
3	1.86137	4967.8	54402.9	71.59
4	2.57966	1434.2	157821	108.13

Table 2: The threshold current for unpolarized modes without frequency spread.

Coupled?	I_{th} [mA]			
	mode 1	mode 1,2	mode 1-3	mode 1-4
no	25.8	25.8	25.8	25.8
yes	28.8	28.8	28.8	28.8

the HOMs are damped fast and a large current is required to deposit enough energy into the HOMs to disturb the beam motion. Thus the cavity should be made so that only the fundamental mode has a very high Q value and all other HOMs have low Q values. In addition to small Qs we can also adjust the lattice to have a small T^*_{12}. But this approach does not always work when there are many cavities because it is not always possible to minimize T^*_{12} for every cavity simultaneously. One example where this is possible is the case of polarized cavities with a fully coupled optics. There we arrange all modes either in x ($\theta_\lambda = 0$) or in y direction ($\theta_\lambda = \frac{\pi}{2}$), which includes the case of unpolarized HOMs for which θ_λ can be chosen arbitrarily. And we couple the x component of a transverse momentum into a y offsets after one turn ($T_{12} = 0$) and vice verse ($T_{34} = 0$). For all cavities this leads to $T^*_{12} = 0$, so that Eq. (1) clearly does not hold. Formulas that also hold in this case are analyzed in [3].

In the following simulations we use the Q values and shunt impedances that were computed for unpolarized 7-cell cavities of the TESLA type [4]. It is not expected that these values change very much when the cavity is changed to a polarized design, however this is currently being analyzed and will be reported in a future paper.

There are different conventions in the definition of $(R/Q)_\lambda$. In the linac definition $(R/Q)_\lambda$ is twice as large as that in the circuit definition. We consistently use the circuit definition. Furthermore $(R/Q)_\lambda$ is sometimes defined with units of Ω/m^2, and sometimes with units of Ω. The conversion between the two is given by

$$\left(\frac{R}{Q}\right)_\lambda [\Omega] = \left(\frac{c}{\omega_\lambda}\right)^2 \left(\frac{R}{Q}\right)_\lambda [\Omega/\mathrm{m}^2] \tag{3}$$

In Tab. 1 both units are shown, but in all subsequent tables we only show values in Ω/m^2.

2 Tracking Results

2.1 Unpolarized HOMs without HOM-frequency spread

Table 2 shows what threshold current can be expected for the x-ray ERL if unpolarized HOMs are used which do not have any frequency spread for the more than 300 cavities. This result demonstrates that a coupled optics does not increase the threshold current significantly when the HOMs are not polarized. All 4 modes of Tab. 1 were used in this simulation. It turns out that using fewer modes does not change the simulation result significantly in this case, which only requires a simulation in the x direction. Since this accelerator should accelerate 100mA, it is clear that means of suppressing BBU is required.

2.2 Unpolarized HOMs with HOM-frequency spread

One strategy to increase the threshold current for a long linac is to avoid that contributions to BBU from different cavities add up coherently. This can be done by introducing a random distribution of HOM frequencies by fabricating each cavity slightly differently, as for example analyzed in [5]. In our simulations we randomized the HOM frequencies according to a Gaussian distribution with an rms width σ_f. The σ_f usually ranges from 1MHz to 10MHz. Different seeds of of the random distribution of HOM frequencies leads to different threshold currents. The resulting random distribution of threshold currents has the rms width σ_I which we calculate by simulating 500 different seeds. Examples of threshold distributions are shown later one in this paper.

Table 3: The threshold current for unpolarized modes with frequency spread.

Δf[MHz]	σ_f[MHz]	$I_{\rm th} \pm \sigma_I$ [mA]			
		mode 1	mode 1-2	mode 1-3	mode 1-4
0	10	427.7 ± 71.1	422.1 ± 70.7	418.1 ± 68.2	405.5 ± 68.2

Table 3 shows the results for the x-ERL. We have chosen a rms frequency spread of 10MHz and have used the HOMs of Tab. 1. The comparison of simulations with 1, 2, 3 and 4 modes shows that a limited number of modes are sufficient for this simulation. Later in this paper we describe a study of the required frequency spread and show why 10MHz has been chosen here.

In order to simulate the randomization of the HOM's frequencies, we use a Gaussian distribution function with desired frequency spread width σ. The problem with this approach is the unignorable statistical fluctuations due to the limited number of HOMs. As we can see in Fig. 1, two simulations scanning the same range of frequency spread give totally different curves for two different seeds of the random frequency distribution.

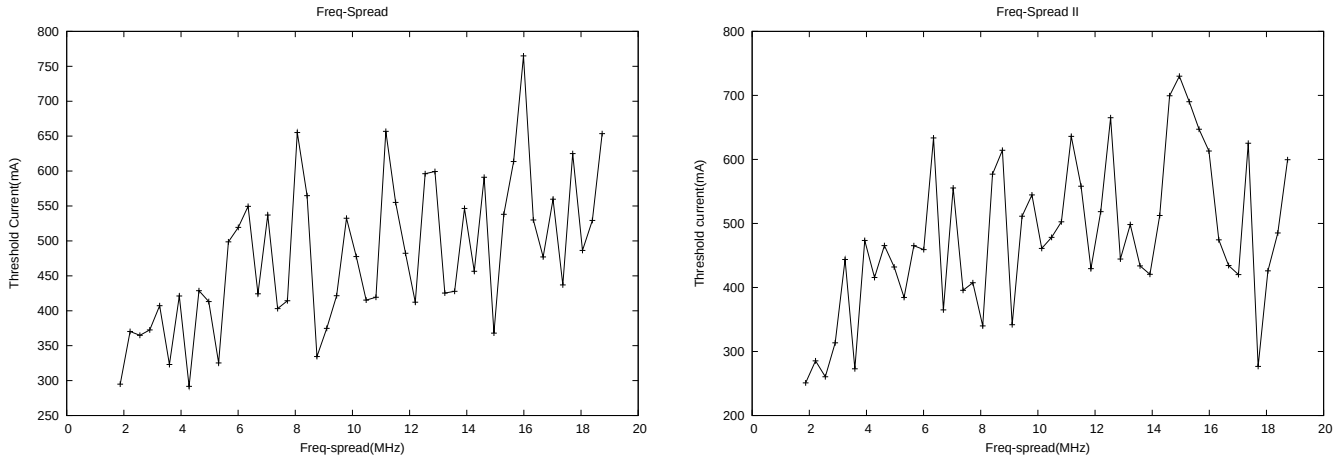

Figure 1: The threshold current as a function of frequency spread for two examples of random seeds for the HOM frequency distribution.

But this fluctuation can be diminished by calculating the threshold current for the same frequency spread many times, in our simulation 500 times, and find the average threshold current, as well as its distribution and rms spread. Fig. 2 shows that the average threshold currents and the width of the threshold current distributions form smooth curves. We can conclude from these curves that a 10MHz frequency spread is reasonable because the average threshold current starts to saturate at this frequency spread.

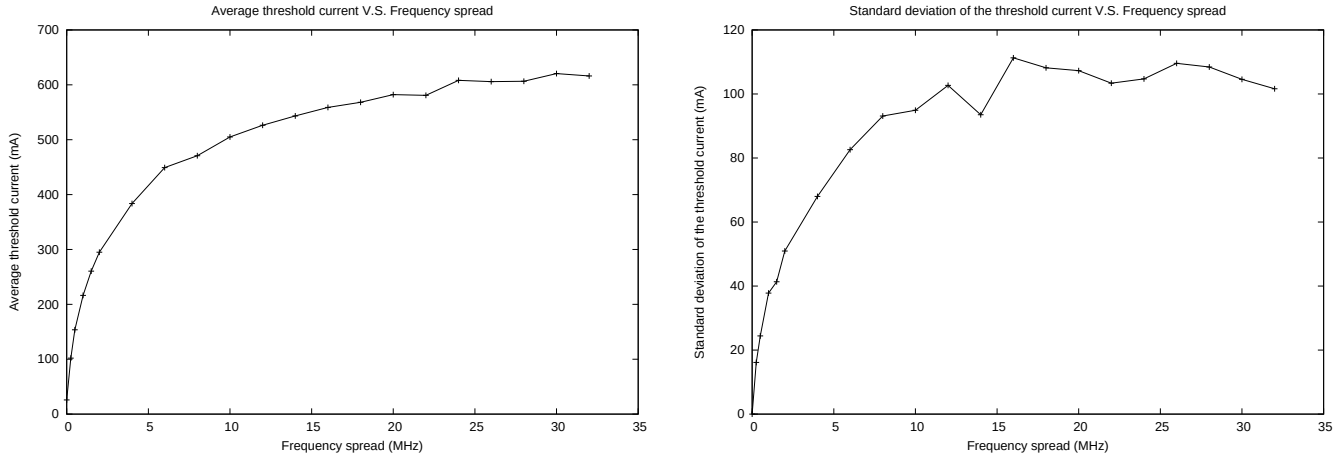

Figure 2: The threshold current and its standard deviation v.s. frequency spread

Table 4 shows how the threshold current depends on frequency spread. Only the first HOM of Tab. 1 was used

Table 4: Threshold current for different rms frequency spread σ_f.

σ_f(MHz)	$I_{\rm th}$ (mA)	σ_I
0	25.84	0.0
0.25	101.98	16.13
0.5	153.66	24.43
1.0	216.35	37.81
1.5	260.52	41.34
2	294.97	50.94
4	383.62	68.00
6	449.14	82.60
8	470.76	93.11
10	505.05	94.90
12	526.35	102.69
14	543.37	93.50
16	558.84	111.29
18	568.10	108.18
20	582.16	107.29
22	580.88	103.37
24	608.19	104.72
26	605.88	109.58
28	606.48	108.42
30	620.58	104.56
32	616.16	101.64

in these simulations. The standard deviations of the threshold current distribution were obtains as the root mean square of the distribution shown in Fig. 3.

The distribution of frequencies for the simulation with 4 modes in Tab. 3 is shown in Fig. 4.

2.3 Polarized HOMs without HOM-frequency spread

A HOM with a polarization angle θ_λ can only kick the beam in that direction. In a circular symmetric cavity, a HOM can kick in any direction. This situation can be described as a linear combination of two degenerate HOMs with frequency $\omega_x = \omega_y$, one being polarized in x the other in y direction.

By manipulating the shape of the RF cavity we can lift the degeneracy and obtain different frequencies for the x and y direction. Then one way to raise the threshold current is to introduce x/y coupling into the lattice. If the HOMs in x and y direction have different frequencies, the beam motion will have different characteristic frequencies in these two directions. Therefore the kick from the HOMs in x direction will be less destructive if we can manipulate the lattice so that this momentum change will cause a displacement in y direction instead of in x direction when the bunch returns to the same cavity. Since the frequency of the x and y modes are different, the beam oscillation in x produced during the first turn does not have the correct frequency to excite the y mode resonantly during the second pass.

Since Eq. (1) leads for this case has $T_{12}^* = 0$, an extremely large threshold current would be expected when different HOMs can be considered independently. It has thus been argued (for example in [6]) that a separation of HOM frequencies by more than their resonance width, i.e. a few MHz, would make modes independent and extremely large threshold currents can be expected. Our simulations prove otherwise. Even for extremely large mode separation of 60MHz, the threshold current only increased by only about a factor of four, which means the two modes couple to each other and cannot be treated separately even with very significantly different frequencies. A theoretical explanation of this effect can be found in [3].

If we use the four main modes and separate x and y polarization modes by 60MHz as shown in Tab. 5, we obtain the data listed in Tab. 6. Later in this paper we will describe a study of the required frequency separation and show why 60MHz has been used here. Our simulation with 2, 4, 6 and 8 modes show that using a limited number of modes for this simulation should be sufficient.

In the simplified theory that leads to Eq. (1), we know that a large Q_λ will lead to a small threshold current. If we apply full x/y coupling and use polarized modes, $T_{12}^* = 0$ and this formula is not applicable, however the efficiency of the x/y coupling method in increasing the threshold current is still determined by Q_λ.

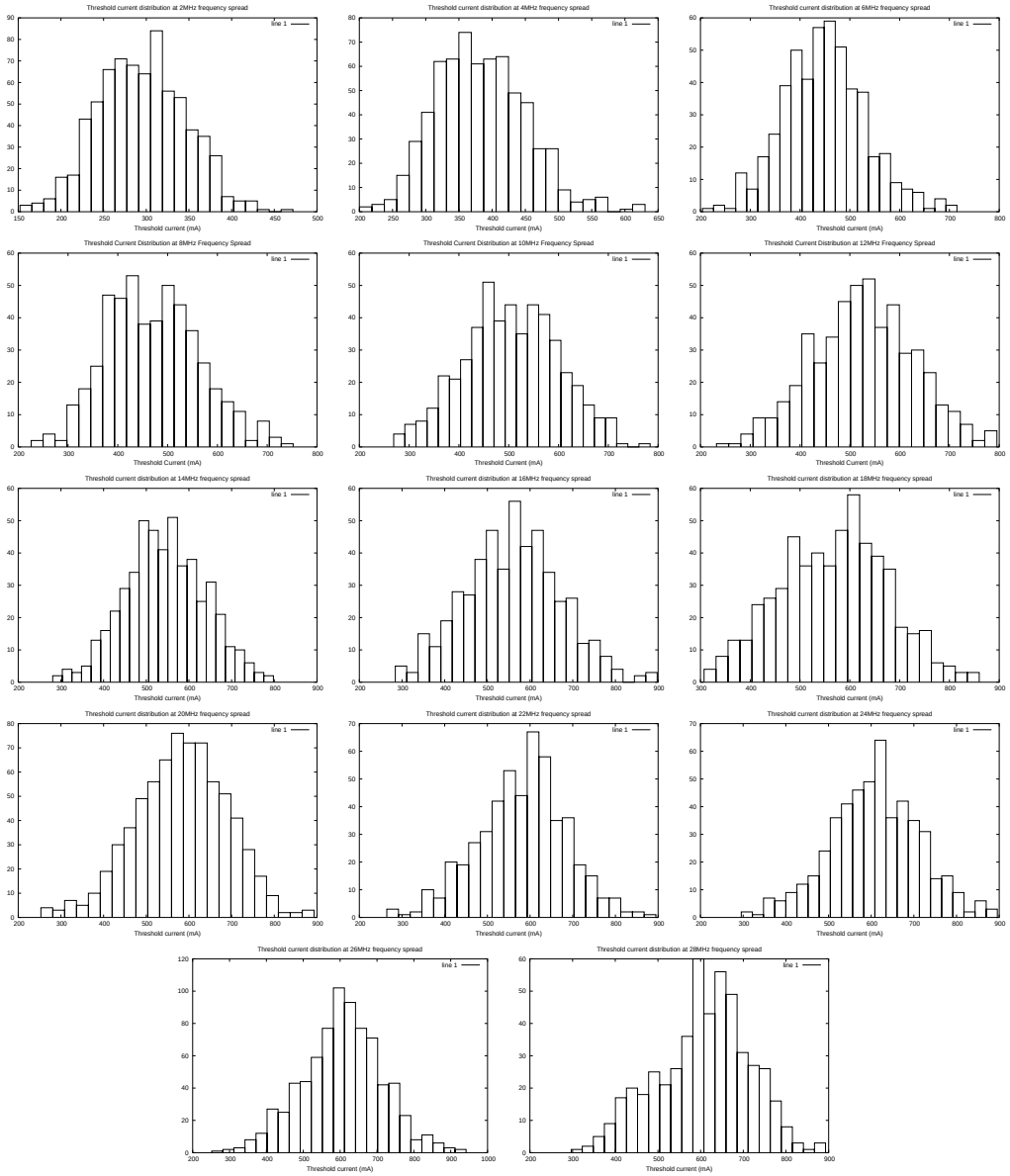

Figure 3: The threshold current's distribution for different frequency spreads: in the order from top right to bottom left 2, 4, 6, 8, 10, 12, 14, 16, 18, 20, 22, 24, 26, 28MHz.

Table 5: The eight most relevant polarized HOM modes.

	f_λ(GHz)	Q_λ	$(R/Q)_\lambda[\Omega/\mathrm{m}^2]$	θ_λ
f_1	1.87394	20912.4	84409.3	0
f_2	1.81394	20912.4	84409.3	$\pi/2$
f_3	1.88173	13186.1	21629.3	0
f_4	1.82173	13186.1	21629.3	$\pi/2$
f_5	1.86137	4967.8	54402.9	0
f_6	1.80137	4967.8	54402.9	$\pi/2$
f_7	2.57966	1434.2	157821	0
f_8	2.51966	1434.2	157821	$\pi/2$

Table 6: The threshold current for polarized modes without frequency spread.

Δf[MHz]	σ_f[MHz]	I_{th} [mA]			
		mode 1,2	mode 1-4	mode 1-6	mode 1-8
60	0	125.7	122.7	118.9	117.6

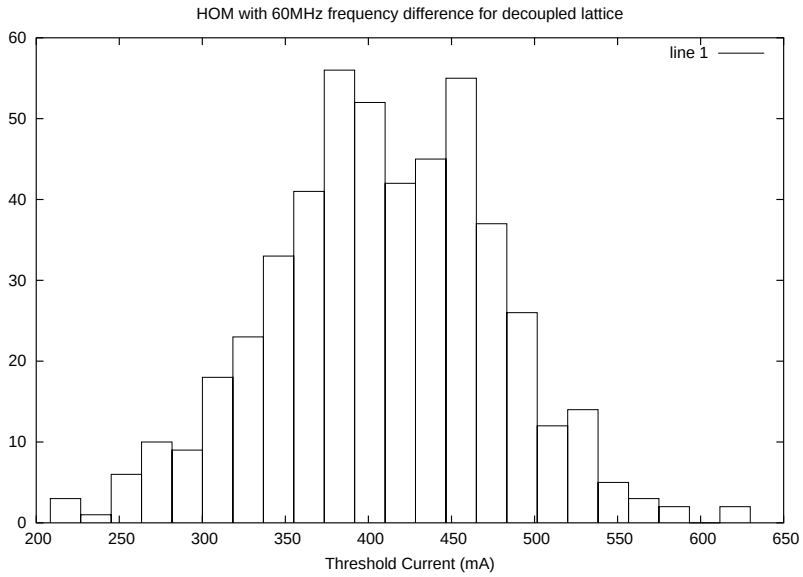

Figure 4: The threshold current's distribution for the decoupled lattice with 10MHz frequency spread

In [3] it is derived that with

$$\mathcal{K}_\lambda = et_b \left(\frac{R}{Q}\right)_\lambda$$
$$\epsilon_\lambda = \frac{\omega_\lambda t_b}{2Q_\lambda}$$

an approximation that assumes two modes with equivalent $(\frac{R}{Q})$ and Q in one cavity and with small coupling, i.e. for $T_{12}^* \neq 0$, leads to

$$I_{\rm th} = -\frac{\epsilon_\lambda}{\mathcal{K}_\lambda}\frac{1}{D_{\lambda\lambda}\sin\omega_\lambda t_r} \qquad D_{\lambda\lambda}\sin\omega_\lambda t_r < 0\ .$$

For strong coupling, i.e. for $T_{12}^* \neq 0$, one obtains

$$I_{{\rm th}\mu}^2 = \frac{2\epsilon_\mu}{\mathcal{K}_\mu\mathcal{K}_\nu}\frac{\cos\omega_\mu t_b - \cos\omega_\nu t_b}{D_{12}D_{21}\cos\frac{\omega_\mu t_b}{2}\sin\frac{\omega_n u t_b}{2}\sin 2\omega_\mu t_r}\ .$$

So for two modes with similar Q_λ, $(R/Q)_\lambda$, and ω_λ, the ratio of the threshold current with and without coupled optics is proportional to $\sqrt{1/\epsilon_\lambda} \sim \sqrt{Q_\lambda}$. While this is a very rough approximation of a linac with more than 300 cavities, each having much more than 2 HOMs, Tab. 7 and Fig. 5 show that the advantage of introducing coupling into the lattice will get smaller with lower Qs, roughly with $\sqrt{Q}$.

In order to study the effect of frequency separation on the threshold current alone, we use mode 1 of Tab. 5 and vary the frequency of mode 2 from 1.77394GHz to 1.97394GHz. No frequency spread is applied in this case.

In Fig. 6 one can see that the threshold current saturates at about ±30MHz frequency separation. Without frequency spread the threshold current is very sensitive to the frequency difference of the two polarized modes when a fully coupled lattice is used. But even when the two HOM frequencies are very far separated, the threshold current is only increased by about a factor of five.

2.4 Polarized HOMs with HOM-frequency spread

The simulations with polarized modes and a coupled optics have lead to an increase in threshold current by about a factor of 4, and the introduction of a 10MHz HOM frequency spread has increased that current by about a factor of 20. Here we will show how much the threshold current is increased when both measures are taken simultaneously. Whenever we apply a frequency spread in our simulation, we make sure that the frequency separation of x and y polarized HOMs is more than $6\sigma_f$. Therefore the frequencies of the two modes are well separated and the coupled lattice works effectively under condition.

Table 7: The advantage of polarized modes with coupling as a function of Q.

Q	$\sqrt{Q}$	I_{dc}(mA) Decoupled	I_c(mA) Coupled	I_c/I_{dc}
4900	70	109.1	365.46	3.350
6400	80	83.55	289.85	3.469
8100	90	66.07	236.25	3.576
10000	100	53.56	196.56	3.670
12100	110	44.39	166.31	3.746
14400	120	37.37	142.68	3.818
16900	130	31.84	123.87	3.890
19600	140	27.51	108.63	3.949
20912	144.6	25.80	102.56	3.975
22500	150	24.01	96.09	4.002
25600	160	21.14	85.66	4.052
28900	170	18.77	76.87	4.095
32400	180	16.76	69.40	4.141
36100	190	15.07	62.99	4.180
40000	200	13.62	57.45	4.218

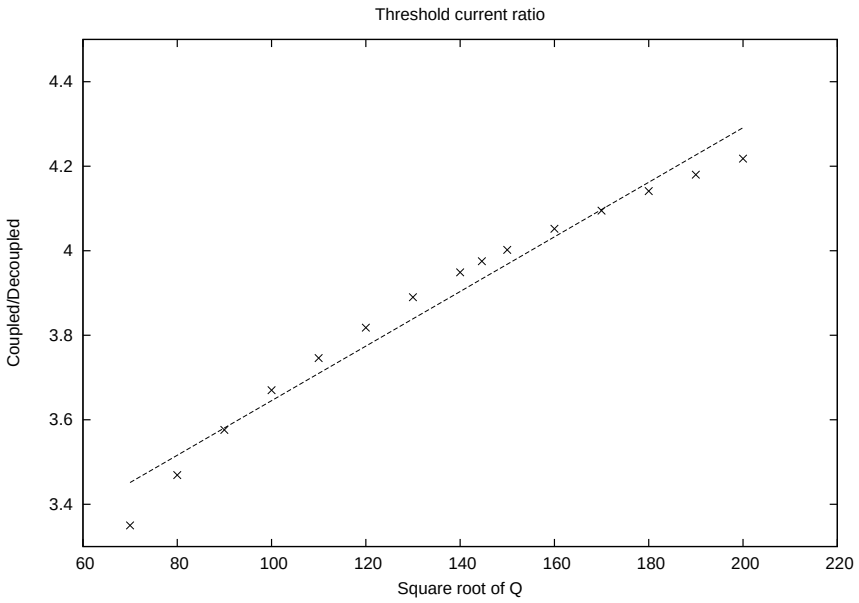

Figure 5: The performance of the coupling method with respect to $\sqrt{Q}$

Table 8: The threshold current for polarized modes with frequency spread.

Δf[MHz]	σ_f	$I_{\rm th} \pm \sigma_I$ [mA]			
		mode 1,2	mode 1-4	mode 1-6	mode 1-8
60MHz	10MHz	2419.5 ± 432.0	2227.0 ± 380.0	1923.2 ± 317.0	1881.3 ± 297.0

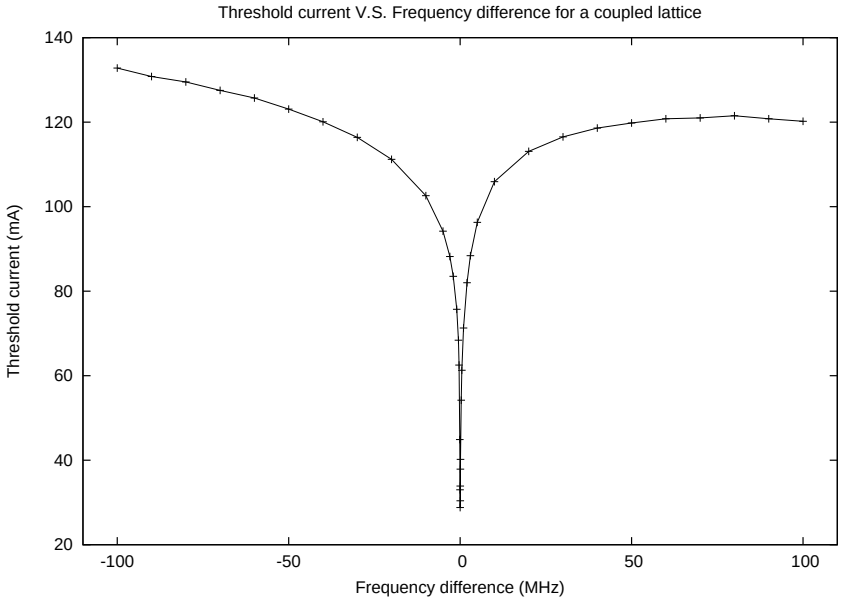

Figure 6: The effect of the difference between the two HOM frequencies

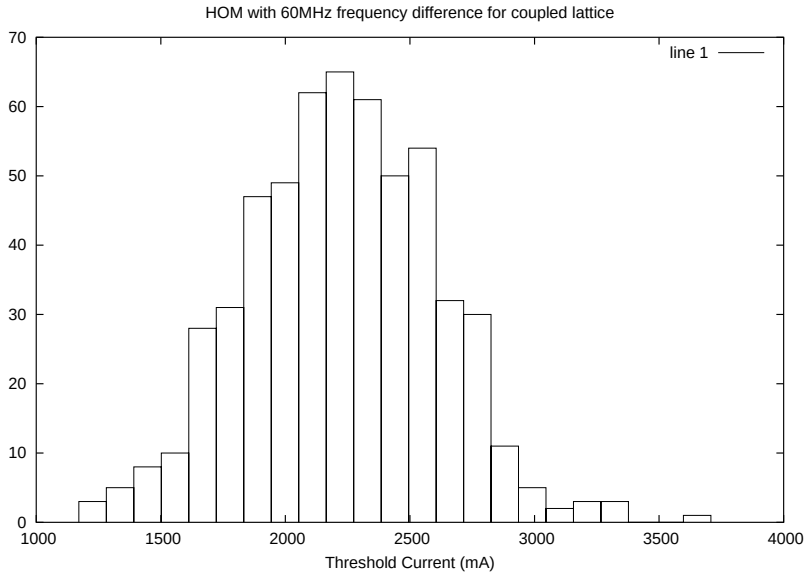

Figure 7: The threshold current's distribution for the coupled lattice with 10MHz frequency spread

The results for the x-ray ERL are shown in Tab. 8.

The distribution of frequencies for the simulation with 8 modes is shown in Fig. 7.

Figure 8 shows a comparison of the threshold currents and the width of their distribution for the for cases: (a) no frequency spread and no coupled optics, (b) frequency spread of 10MHz but no coupled optics, (c) no frequency spread but a coupled optics with polarized modes of 60MHz frequency separation, (d) 10MHz frequency spread as well as 60MHz frequency separation.

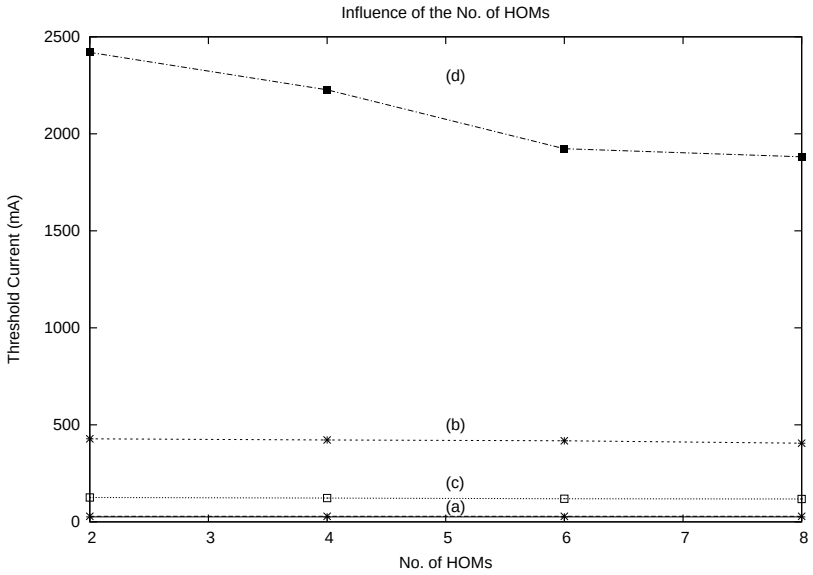

Figure 8: The threshold currents and their distribution for the following combinations of mode frequency separation Δf and frequency spread σ_f: (a) 0, 0, (b) 0, 10MHz, (c) 60MHz, 0, (d) 10MHz, 60MHz.

Since a frequency spread increases the threshold current by about a factor of 20 whereas coupling with mode polarization yields only about a factor 5, one can conclude that the interference between different cavities is more destructive than the interference between the HOM modes in different orientations. Thus the critical part is to introduce frequency spread among the HOM frequencies on top of using polarized modes. This leads an increase of the threshold current by about a factor of 100, indicating that the effects of frequency separation and frequency spread are nearly independent from each other.

To analyze what mode separation is needed, we simulated the threshold current under a frequency spread of $\sigma_f = 10$MHz by averaging over 500 random seeds of HOM frequencies. The result in Fig. 9 shows that a frequency separation of about 60MHz is beneficial, and that separations below 25MHz do not lead to significant improvements. The lower curve includes four HOMs while the one above it includes the two main HOMs. We conclude that the two main HOMs are paramount in determining the threshold current.

2.5 Study on the influence of the phase advance on the threshold current

By adjusting the phase advances of the x and y beta function we can change the elements in the transfer matrix $\mathbf{T}$. Therefore we can find a pair of phase advances to optimize the threshold current. In Fig. 10 we can see that the maximum threshold current we can get by adjusting the phase advances is about 150 mA for the x-ray ERL when no frequency spread but mode polarization is used. This has to be compared to the 125.7mA listed in Tab. 6, indicating the the betatron phase is not a strongly effective variable to optimize the threshold current in the x-ray ERL.

2.6 A note on lattice changes

The tracking results that have been presented so far have been computed with a linac lattice that has been superseded by a new design. To illustrate how changing the linac lattice can influence the threshold current, we show the results of a few simulations that were done with the new linac lattice.

The threshold currents are shown in Tab. 9 and the threshold current distribution is shown in Fig. 11.

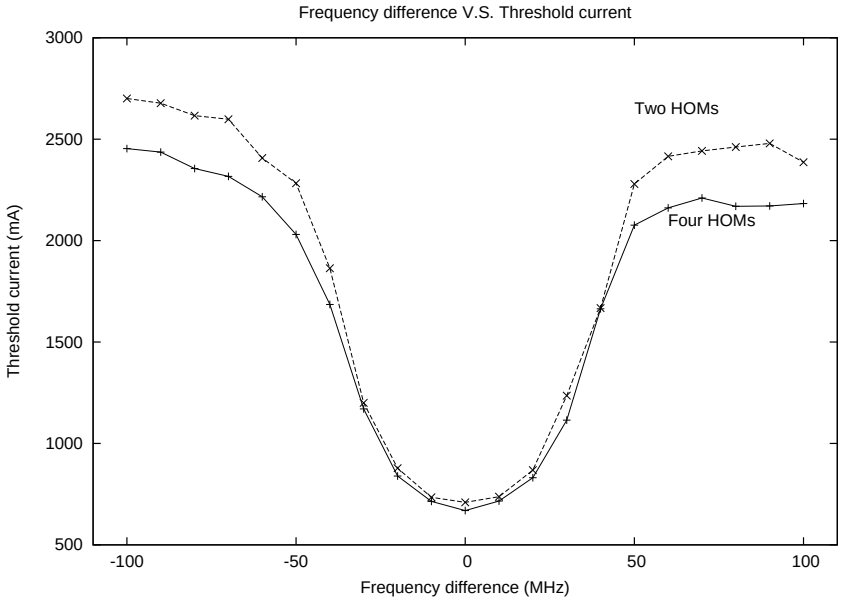

Figure 9: The effect of the difference between HOM frequencies with frequency spread

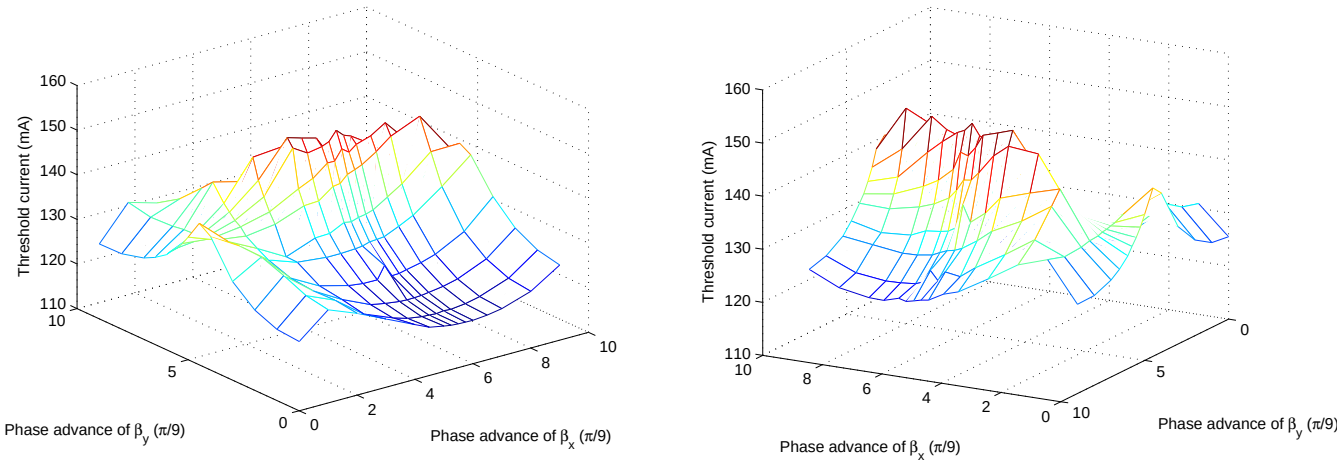

Figure 10: Threshold current v.s. x and y betatron phase advances of without frequency spread but with coupling and mode separation of 60MHz.

Table 9: The threshold current for unpolarized modes without frequency spread.

Coupling?	Δf[MHz]	σ_f[MHz]	$I_{\rm th}$ [mA]			
			mode 1-2	mode 1-4	mode 1-6	mode 1-8
no	0	0	21.9	21.9	21.9	21.9
yes	60	0	95.9	94.0	90.1	90.2
yes	60	10	2076 ± 341	1900 ± 290	1623 ± 244	1591 ± 223

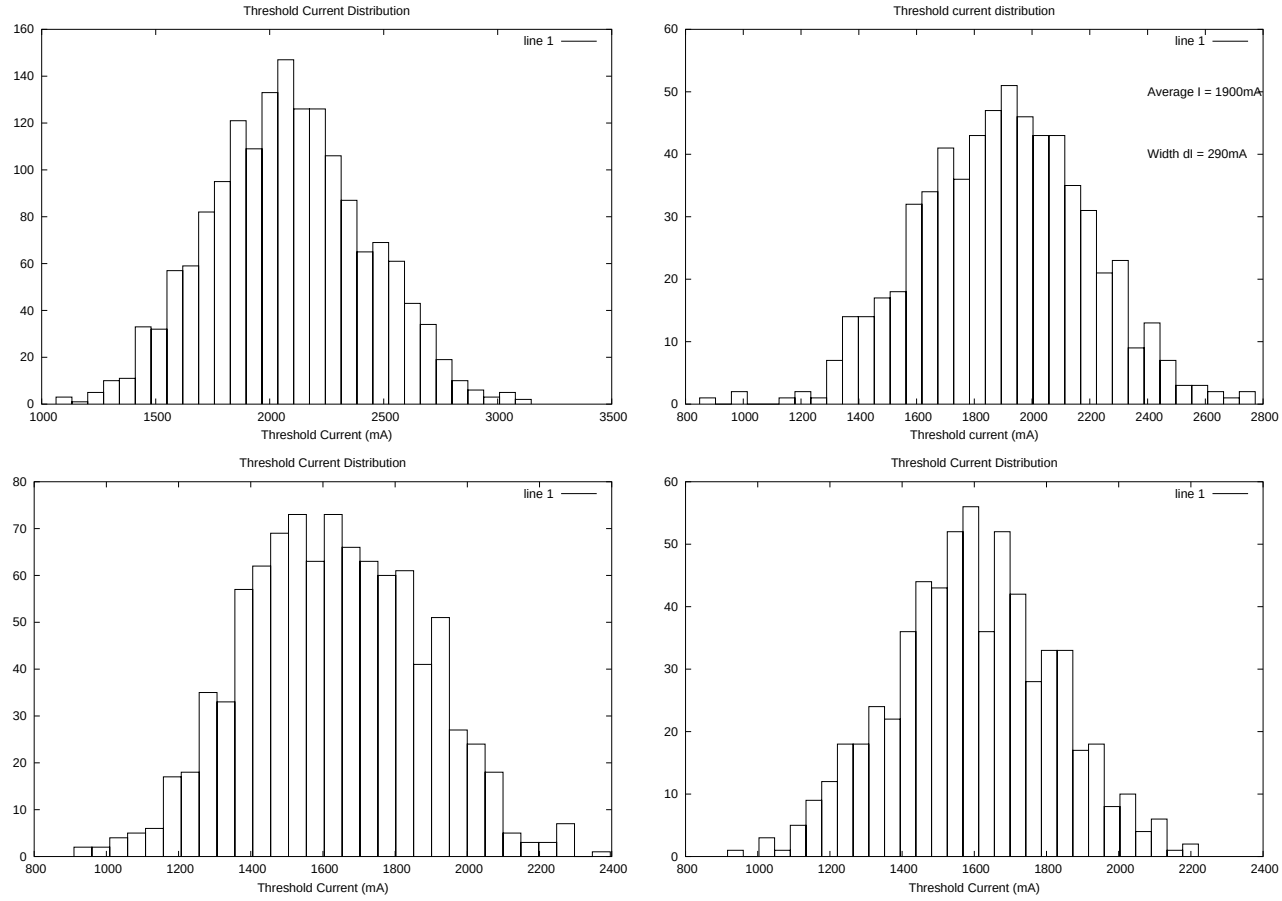

Figure 11: The threshold current's distribution for the new linac lattice with 10MHz frequency spread, mode separation of 60MHz, coupling and with 2, 4, 6, and 8 modes in the order from top left to bottom right.

3 Acknowledgments

We thank Ivan Bazarov for providing some of the simulation codes and his insightful comments. We also thank Matthias Liepe for providing the HOM parameters used in our simulation.

References

[1] E. Pozdeyev, "Regenerative multipass beam breakup in two dimensions", Phys. Rev. ST AB **8**, 054401 (2005).

[2] G.H. Hoffstaetter and I.V. Bazarov, "Beam-breakup instability theory for energy recovery linacs", Phys. Rev. ST AB **7**, 054401 (2004).

[3] G.H. Hoffstaetter, I.V. Bazarov, C. Song, "Recirculating BBU thresholds for polarized HOMs with optical coupling", Phys. Rev. ST AB submitted (2005).

[4] M. Liepe, "Conceptual Design of the Cavity String of the Cornell ERL Main Linac Cryomodule", Proceedings SRF03 (2003)

[5] I.V. Bazarov, G.H. Hoffstaetter, Multi-pass beam-breakup: Theory and Calculation, Report Cornell-ERL-04-7 and Proceedings EPAC04, Lucerne/CH (July 2004)

[6] E. Pozdeyev, "BBU Observations at the JLAB ERL", Presentation during the ERL workshop, TJNAF (March 2005).